



Received: 09-11-2023

Accepted: 19-12-2023

ISSN: 2583-049X

## Computational Analysis of Transient Magnetohydrodynamic Micropolar Fluid Flow over a Permeable Substrate

<sup>1</sup> Hamed Fatai Akangbe, <sup>2</sup> Akanbi Olumuyiwa Olawale

<sup>1</sup> Department of Mathematical Sciences, Olabisi Onabanjo University, Ago-Iwoye, Nigeria

<sup>2</sup> Department of Mathematics and Statistics, Federal Polytechnic, Ilaro, Nigeria

Corresponding Author: **Hamed Fatai Akangbe**

### Abstract

The present study delves into the transient phenomenon of a magneto-micropolar fluid configured in a permeable material device. This analysis suits flow in reservoirs, metal casting, and composite manufacturing, petroleum industry, particularly in modelling fluid flow in porous rocks during enhanced oil recovery operations. The understanding of micropolar fluid dynamics in permeable media could be applied to model groundwater flow and contamination remediation strategies. The boundary layer, Boussinesq approximations, and some appropriate assumptions are used to formulate the mathematical model for the present problem. The model consists of the effects of the non-

constant thermophysical properties, viscous and Joule heating properties. The highly coupled nonlinear equations are solved numerically using the unconditionally stable Runge-Kutta Fehlberg method and the shooting techniques. The consequence of the numerical analysis is depicted in various graphs and tables for proper deliberation of results. The results indicate a depreciation in the momentum and thermal boundary structures as the transient term enhances. The porosity and the magnetic field parameters cause a decelerating motion but raise the thermal distribution as the material term boosts the fluid flow.

**Keywords:** Micropolar Fluid, Magnetohydrodynamic, Permeable Sheet, Non-Constant Viscosity

### 1. Introduction

It is no gainsaying that non-Newtonian fluids play crucial roles in various fields of science, engineering and technology ranging from oil drilling, food production, drug manufacturing, paint rheology, medical and bio-medical processes, etc. In light of this, many researchers have been encouraged to investigate the flow and heat properties of these fluids for prediction in practical situations. In addition, the need to enhance industrial productivity and engineering device performance has motivated various studies on the dynamics of non-Newtonian fluids. These fluid phenomena are a good tool in engineering, biological science, geophysics, and pharmaceutical processes (Khan *et al.*, 2019 <sup>[16]</sup>; Fluid flow, including heat transmission overstretching materials, is of utmost relevance in engineering and industrial settings. Such a study is of primary importance as the foundation for designing and optimising continuous material-forming processes like polymer extrusion, wire drawing, textile manufacturing, fibre spinning, etc. Improving product quality, process efficiency, and industrial output all depend on an understanding of the nuances of fluid behaviour under these conditions (Makinde *et al.*, 2015; Hsiao, 2016; Khan *et al.*, 2016; Fatunmbi *et al.*, 2020; Fatunmbi and Okoya, 2020) <sup>[19, 11, 15, 6, 8]</sup>.

It is important to remark that various models of non-Newtonian fluids have been developed because no single model has the properties of these fluids in its constitutive equations. These models include micropolar fluid, Casson fluid, Gesekus, Prandtl-Eyring, Powell-Eyring models, etc. Of these models, the micropolar fluid stands out due to its ability to simulate complex and complicated fluids of microstructures, rigid particles and non-symmetric stress tensors. This fluid model was developed by Eringen (1964, 1966 <sup>[3]</sup>, 1972 <sup>[4]</sup>). Its relevance has inspired various scholars to investigate its characteristics. Das *et al.* (2016) <sup>[2]</sup> engaged in Lie group analysis to evaluate the micropolar fluid properties over a vertical plate with slip effects chemical reactions. Tripathy *et al.* (2016) simulated the flow of a micropolar fluid in a porous medium. The numerical study incorporated the influence of uneven heat source and concluded that a shrinking structure of the momentum layer exists with a higher magnitude of the porosity and magnetic field terms. Rashad *et al.* (2019) <sup>[21]</sup> discussed such a concept in a porous cylinder consisting of nanoparticles, whereas Jain and Gupta (2019) <sup>[13]</sup> pointed out the usefulness of the micropolar fluid in various industrial processes such as liquid crystal solidification, exotic lubricants, colloidal and suspension solution, extrusion of polymer, etc. Fatunmbi and Okoya (2021) <sup>[5]</sup> examined the combined properties of electric-magnetic micropolar fluid flow

and heat transfer influenced by dissipative heating and variable physical characteristics in a porous medium. Gumber *et al.* (2022) <sup>[10]</sup> investigated micropolar fluid motion coupled with heat transfer analysis in the presence of thermal radiation, surface mass flux and hybrid nanoparticles. The numerical simulation via the shooting and R-K-F method showed that heat transfer is larger for injection than for suction.

The boundary layer transport and heat transmission in porous devices are of interest in many fields, for instance, agriculture, where irrigation is practiced; geology, in biomedical engineering, such as blood flow in the brain and body, etc. To improve the effectiveness and sustainability of these processes, it is essential to have a deeper understanding of the dynamics at play when micropolar fluids interact with inclined, permeable surfaces. Additionally, magnetic fields can be employed to control fluids' motion and heat distribution and in other engineering works. For instance, magnetic fields are applicable in drug targeting systems for biological systems, the control of ferrofluids in aerospace, treat cancer cells, etc. Kameel *et al.* (2014) <sup>[14]</sup> developed a micropolar fluid flow model over an isotropic porous device using the intrinsic volume averaging idea in light of these applications. Jabeen *et al.* (2020) <sup>[12]</sup> inquired about Newtonian fluid flow passing a porous medium membrane subject to viscous and Joule heating using a semi-analytic method. Fatunmbi *et al.* (2020) <sup>[6]</sup> scrutinised the transport of heat-mass of MHD micropolar passing a nonlinearly elongating sheet in a material device filled with pores under the influence of slips. The authors engaged an iterative spectral quasi-linearization method and reported a collapse of the momentum boundary structure with a rise in the nonlinear power index factor.

The above researchers, however, assumed that the flow is steady in their investigations without taking cognisance of unsteadiness in the flow pattern, which usually occurs in real-life situations. In practical situations, however, unstable flow conditions must be considered because the flow becomes time-dependent due to sudden stretching of the material device or a step change in the temperature or heat flux of the material. In this view, Elbashbeshy *et al.* (2012) engage a numerical instrument via Mathematica software to investigate the similarity solutions of an unsteady exponential plate. Nagaraju and Murthy (2014) <sup>[20]</sup> explored an unsteady flow of a micropolar fluid in a circular cylinder. Nadeem *et al.* (2020) researched the over-the-flow of micropolar fluid passing an exponentially stretching plate subjected to slip properties. Meanwhile, Fatunmbi *et al.* (2022) extended such scenario with entropy generation, several slips, an uneven heat source, and radiation effects. Further, Khan *et al.* (2022) scrutinised an unsteady micropolar fluid over a vertical extending/shrinking sheet with a blend of hybridised nanofluid. The various studies above found that the unsteadiness situations in the fluid flow and heat transfer problems capture the intricate behaviour and effective prediction which were ignored in steady-state investigations. This is especially important in practical settings where time-dependent processes or quick changes in external variables play a significant role. Including porous material opens up a new realm of potential uses in science, engineering, and technology.

The literature examined above and various applications derivable from them have inspired the present investigation. Thus, the current study proposes to explore a numerical means to elucidate the complex phenomenon of micropolar fluid flow where the unsteadiness situation is accounted for. The mathematical model includes the magnetic field term and the interplay between unsteadiness, vortex viscosity dynamics, interactions in porous media, the thermal radiation effect, and weak concentration of the microparticles at the wall. This study applies in various scientific and engineering fields, including geophysics and biomedical engineering, to industrial applications such as food processing, extrusion processes, etc.

**2. Assumptions for Problem Modelling and Governing Equations**

In developing the governing for the current problem, some assumptions must be put in place. In this case, the flow is assumed to be linear and time-dependent. The vivid picture of the configuration of flow and heat dissipation property is depicted in Fig 1. Incompressibility assumption is valid; thermophysical properties change with temperature in a linear fashion, the magnetic field is perpendicular to the motion of the flow, and a weak concentration of the micro-particles is present. Furthermore, the heat region is modelled, assuming that Joule heating, viscous dissipation, and radiative heat sources are present. The Bousnessq assumption is also applied in the momentum equation (2) for the variation of the density in the body force, while the heat distribution at the wall is assumed to be isothermal in nature. Fig 1 shows clearly the sketch of the flow configuration the coordinate axes of flow, and the transverse field.

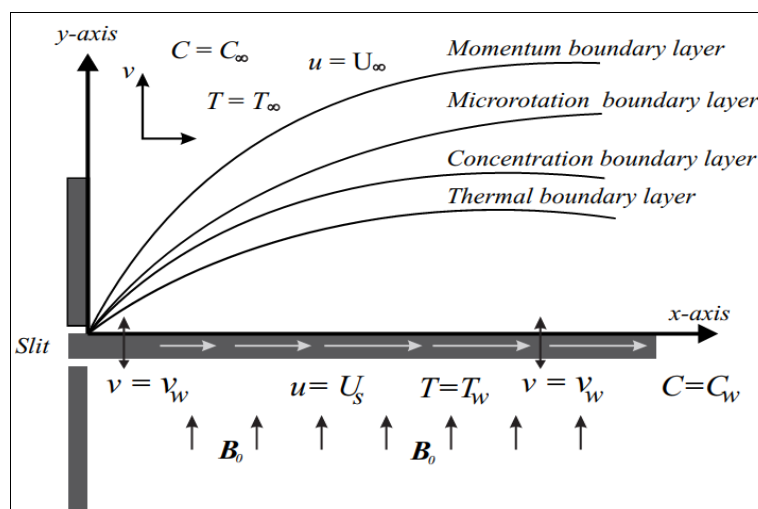


**Fig 1:** Flow geometry

In line with the above assumptions, the equations governing the present problem are:

$$\frac{\partial u}{\partial x} + \frac{\partial v}{\partial y} \tag{1}$$

$$\frac{\partial u}{\partial t} = \frac{1}{\rho_{\infty}} \frac{\partial}{\partial y} \left( \mu \frac{\partial u}{\partial y} \right) + \frac{r}{\rho_{\infty}} \frac{\partial^2 u}{\partial y^2} + \frac{r}{\rho_{\infty}} \frac{\partial \omega}{\partial y} - \left( \frac{\sigma_0 B_0^2}{\rho_{\infty}} + \frac{\mu}{\rho_{\infty}} \right) u + gB(T - T_{\infty}) - u \frac{\partial u}{\partial x} - v \frac{\partial u}{\partial y} + gB_c(N - N_{\infty}) \tag{2}$$

$$\frac{\partial \omega}{\partial t} = \frac{\gamma}{\rho_{\infty} j} \frac{\partial^2 \omega}{\partial y^2} - \frac{r}{\rho_{\infty} j} \left( 2\omega + \frac{\partial u}{\partial y} \right) - u \frac{\partial \omega}{\partial x} - v \frac{\partial \omega}{\partial y} \tag{3}$$

$$\frac{\partial T}{\partial t} + \rho_{\infty} \left( u \frac{\partial T}{\partial x} + v \frac{\partial T}{\partial y} \right) = \frac{1}{c_p} \frac{\partial}{\partial y} \left[ \left( \kappa + \frac{16T_{\infty}^3 \sigma^*}{3k^*} \right) \frac{\partial T}{\partial y} \right] + \frac{(\mu+r)}{c_p} \left( \frac{\partial u}{\partial y} \right)^2 + \frac{\sigma_0 B_0^2}{c_p} u^2, \tag{4}$$

$$\frac{\partial C}{\partial t} + u \frac{\partial C}{\partial x} + v \frac{\partial C}{\partial y} = D_b \frac{\partial^2 C}{\partial y^2} - k_r(N - N_{\infty}) \tag{5}$$

The respective wall constraints are specified as follows:

$$u = u_w, v = V_w, \omega = -n \frac{\partial u}{\partial y}, T = T_w, N = N_w \text{ at } y = 0, \\ u \rightarrow 0, \omega \rightarrow 0, T = T_{\infty}, N = N_{\infty} \text{ as } y \rightarrow \infty. \tag{6}$$

The symbolic description of various terms in the equations listed above are given as follows: T depicts the temperature of the fluid,  $N$  connotes concentration,  $u$  indicates velocity in the direction of  $x$ ,  $v$  illustrates velocity in  $y$  route,  $g$  defines gravitational acceleration,  $B$  shows the coefficient of thermal expansion,  $B_c$  picture coefficient of solutal expansion,  $\kappa$  indicates thermal conductivity,  $x$  and  $y$  are cartesian coordinates,  $\omega$  signifies the microrotatio component,  $n$  indicates boundary surface term,  $u_w$  denotes plate velocity,  $V_w$  picture surface flux,  $c_p$  is named as specific heat capacity,  $B_0$  is known as magnetic field strength,  $\gamma = \left( \mu + \frac{\kappa}{2} \right) j$  signifies the spin gradient viscosity, the subscript  $w$  and  $\infty$  connote wall and upstream conditions respectively.

To change the formulated partial derivations to suitable ordinary derivatives, the approach of similarity techniques is employed. Thus, we introduced some similarity quantities as indicated in equation (7), where  $\eta$  is known as the similarity variable, and prime stands for derivatives with respect to  $\eta$  but  $\theta, f$  and  $\phi$  are the non-dimensional temperature, stream and concentration in that order.

$$\eta = \sqrt{\frac{c}{v(1-\beta t)}} y, \psi = \sqrt{\frac{cv}{(1-\beta t)}} x f(\eta), T = (T_w - T_{\infty})\theta + T_{\infty}, N = (N_w - N_{\infty})\phi, \tag{7}$$

The use of these quantities in (7) in (1-6) results in the validity of (1), whereas (2-6) become

$$(1 + K)f'''' + \alpha \theta' f''' + Kg' + ff'' - Mf' - Daf' + Gr\theta + Gc\phi = 0, \tag{8}$$

$$\left( 1 + \frac{K}{2} \right) g'' + f'g + fg' - 2K(2g + f'') = 0, \tag{9}$$

$$(1 + \delta\theta + Nr)\theta'' + \delta\theta'^2 + (1 + \delta\theta)f\theta' + PrEc(1 + K)f''^2 + PrEc f^2 = 0. \tag{10}$$

$$\phi'' + Sc\phi' - Sc\phi\theta'' - (\zeta\phi) = 0. \tag{11}$$

Similarly, the conditions at the boundary are now

$$f'(0) = 1, f(0) = fw, g(0) = -nf''(0), \theta(0) = 1, \phi(0) = 1 \\ f'(\infty) = 0, g(\infty) = 0, \theta(\infty) = 0, \phi(\infty) = 0. \tag{12}$$

The emerging dimensionless parameters are described as follows:  $K$  denotes the micropolar fluid term,  $\delta$  connotes the thermal conductivity term,  $Pr$  defines the Prandtl number,  $Ec$  defines the Eckert number,  $Sc$  defines the Schmidt number,  $Nr$  defines

the radiation term,  $Gr$  stands for the thermal Grashof number,  $Gc$  depicts the Solutal Grashof number and  $\alpha$  depicts the viscosity parameter.

### 3. Method of Solution

The resulting ordinary differential equations (8-12) designate a boundary value problem, which is a nonlinear coupled one. Thus, the analytical solution is not attainable easily, we have resolved to apply a numerical means via the shooting and Runge-Kutta Fehlberg method to tackle the problem. This method is unconditionally stable and accurate in tackling nonlinear equations, as reported by various authors. Thus, computational codes were written for the governing equations and implemented on the Maple software for the solution. This method has been used by Upreti *et al.* (2018) [23], Gumber *et al.* (2020); and Das *et al.* (2016) [2]. The accuracy of the results is checked by verifying the current results with the related studies in literature under strict limiting conditions, as compiled in Table 1.

### 4. Results analysis and deliberations

For further explanation of the impact of the various emerging terms in relation to the flow fields, some graphs have been plotted and discussed in this section.

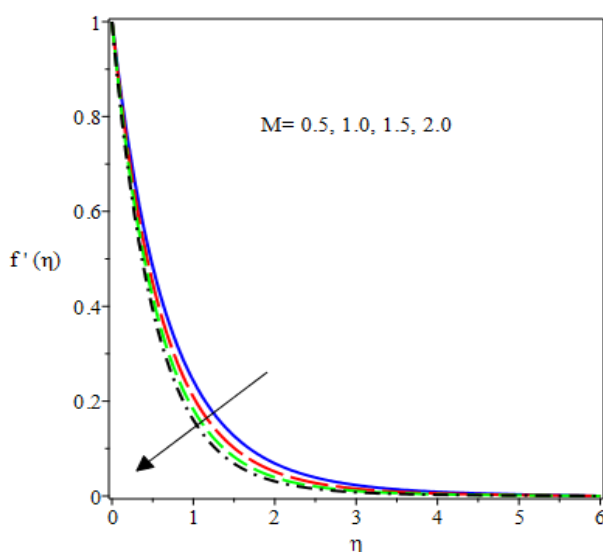


Fig 2: Pattern of velocity profile for  $M$

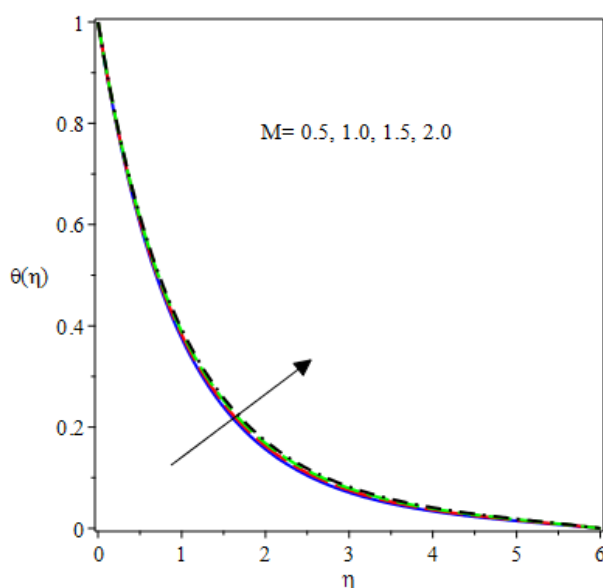


Fig 3: Temperature behaviour for  $M$  values

Fig 2 shows that the magnetic field term  $M$  resists the fluid motion as it rises in strength. The converse occurs in Fig 3 as the thermal region enhances due to higher  $M$ . These reactions manifest because of the Lorentz force imposed on the fluid. It is clearly seen that magnetic field inclusion in the flow of the micropolar fluid can effectively control the flow pattern and the heat distribution as well. The microrotation field is found to be increasing with the action of  $M$ . The boundary layer structure of the microrotation profile continues to enlarge when micro-particles are present, as depicted in Fig 4.

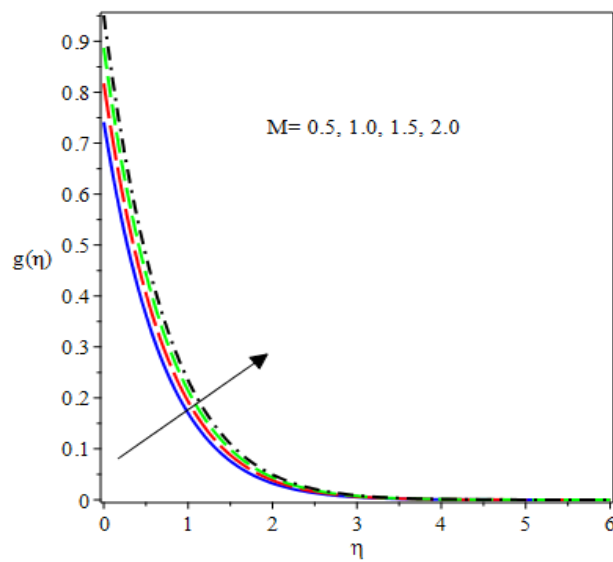


Fig 4: Microrotation profile for  $M$

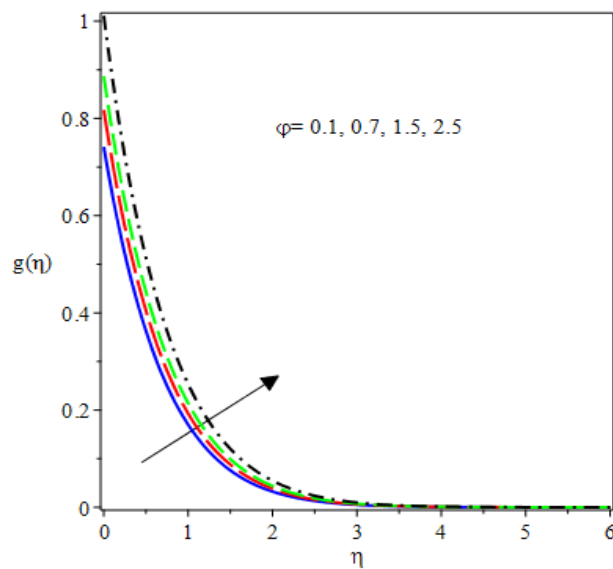


Fig 5: Velocity pattern for porosity term

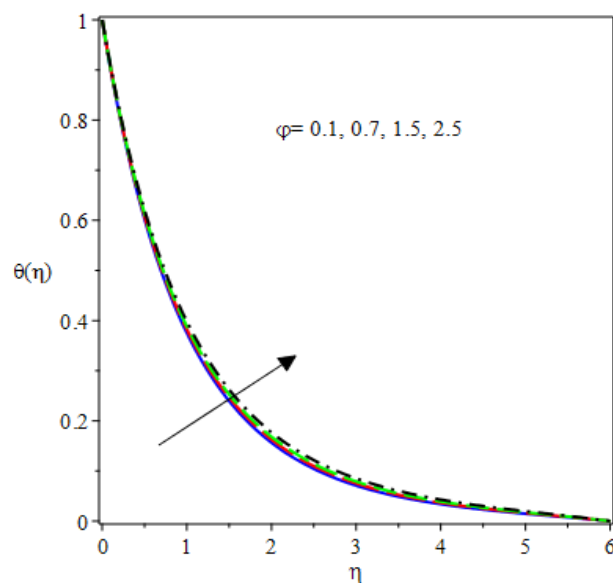
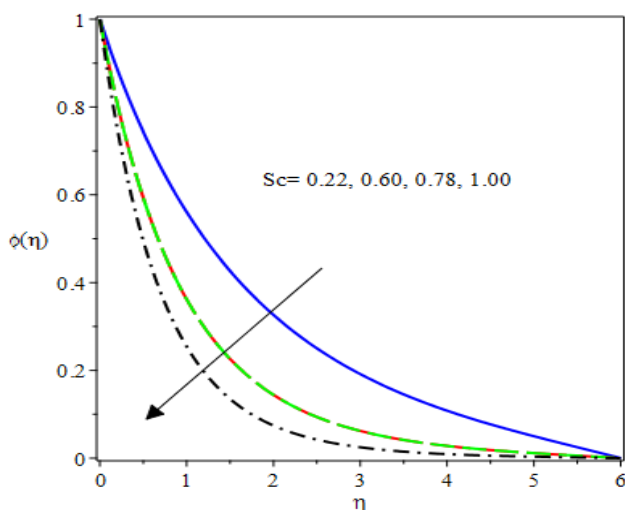
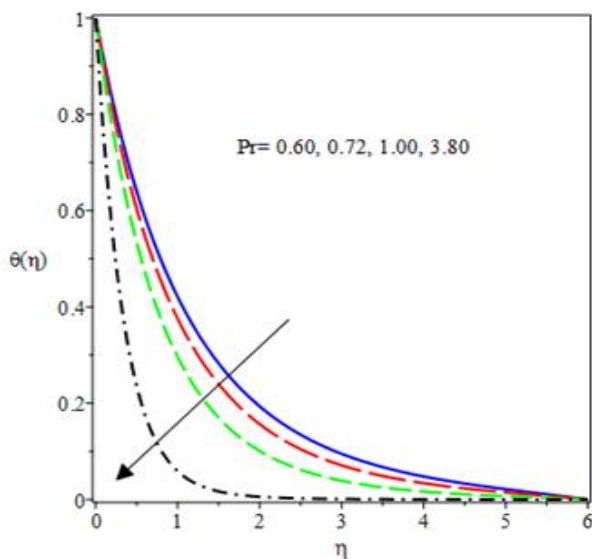


Fig 6: Thermal reaction to variation in porosity



**Fig 7:** Concentration profile for Sc

Fig 5 illustrates the effect of the porosity parameter on the velocity profile. The result indicates that increasing the porosity parameter tightens the porous medium and consequently increases the resistance against the flow, hence decreasing the fluid velocity profile. Fig 6 depicts the temperature profile for various values of the porosity parameter. It is noticed that the temperature profile increases with an increasing porosity parameter. This is because as the fluid flow slows down due to the tightening of the porosity medium, heat is transferred to the fluid from the hot surface, increasing the temperature profile. It is evident in Fig 7 that rising values of Sc result in a depletion in the solute profile. The behaviour of Pr in the thermal vicinity is presented in Fig 8. A depleted structure of the thermal boundary surfaced as Pr enlarges, and such a reaction resulted in a diminished temperature distribution in the heat region, as clearly noted in the graph.



**Fig 8:** Thermal field for diverse Pr

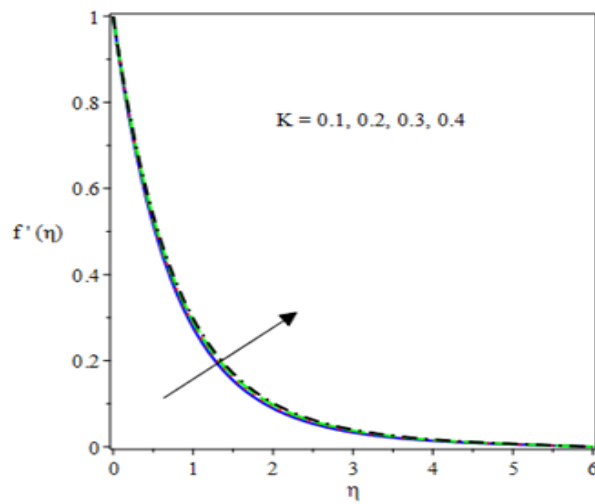


**Fig 9:** Velocity profiles for alterations in  $K$  values

A rise in the velocity profiles and the hydrodynamic structure is found in Fig 9 as  $K$  grows in magnitude. This is so because of the reduction in the dynamic viscosity which lessens the resistance on the fluid motion.

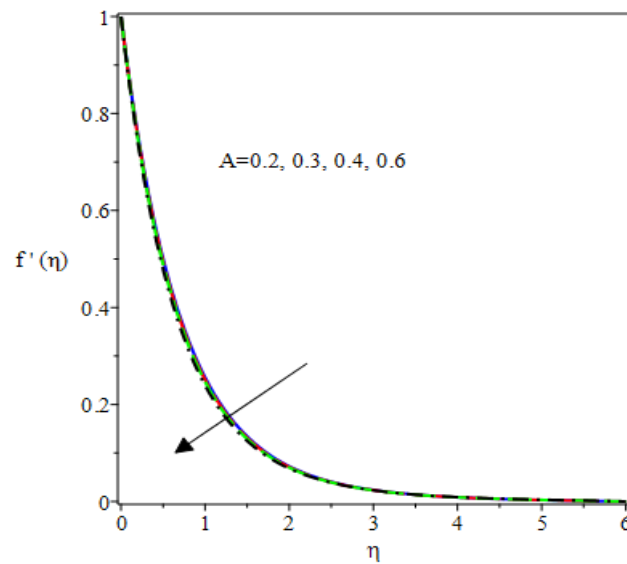


**Fig 10:** Velocity profile for unsteadiness term

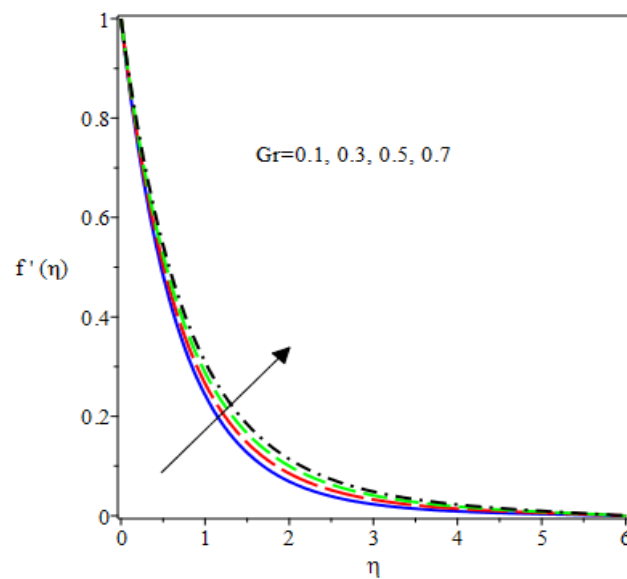


**Fig 11:** Velocity profile for Grashof



The effect of the unsteadiness parameter on the velocity profile is presented in Fig 10. It is noted that increasing the unsteadiness parameter leads to a decrease in the velocity profile. This is due to the thickening of the thermal boundary layer as the unsteadiness parameter increases, which in turn decreases the velocity profile. On the other hand, there is accelerating flow as  $Gr$  rises. This is because the buoyancy force is encouraged by the growth in  $Gr$  while the viscous force is diminished.

### Results verification

To verify the validity and accuracy of the present study, the numerical results for Nusselt number with existing related studies for exceptional cases. The results have been verified by comparing the values of the Nusselt number with the previous data obtained in the literature under some limiting constraints. The present numerical values obtained, as shown in Table 1 from previous works, are in excellent agreement.

**Table 1:** Comparison of  $\theta'(0)$  for variation in  $A, fw, Pr$  and  $Gr$

$A$	$fw$	$Pr$	$Gr$	Ishak <i>et al.</i> (2009)	Musa <i>et al.</i> (2019)	Present study
0	-1.5	0.72	0	0.4570	0.4570	0.457297
		1.00		0.5000	0.5001	0.500017
		10		0.6452	0.6451	0.645160
	0	0.01		0.0197	0.0197	0.112200
		0.72		0.8086	0.8086	0.808834
		1.00		1.0000	1.0000	1.000008
		3.00		1.9237	1.9239	1.923679
		10.0		3.7207	3.7207	3.720671

### 5. Conclusion

The present problem is based on the unsteady motion of magnetized micropolar fluid over a vertical stretching material in a porous device. The flow is configured in a two-dimensional sheet with isothermal heating conditions and chemical reaction terms. The other parameters included in the study are thermal radiation changeable thermophysical properties, A mathematical model is set up for the design of the problem, and the equations are subjected to a numerical solution via the Runge-Kutta Fehlberg method combined with the shooting techniques. The investigation outcomes are shown in various tables and figures to determine the intricate relationship of the physical terms on the transport phenomenon. The investigation reveals that the porous parameter, unsteadiness, and magnetic field terms deplete the flow of the fluid. There is a significant reduction in the surface drag tension as the material and magnetic field terms rise in magnitude. Heat transfer is improved by the micropolar parameter but reduced by the magnetic field term.

### 6. References

1. Ayano MS, Sikwila ST, Shateyi S. MHD mixed convection micropolar fluid flow through a rectangular duct. *Math Prob Eng*, 2018, 1-8.
2. Das K, Acharya N, Kundu PK. MHD micropolar fluid flow over a moving plate under slip conditions: An application of Lie group analysis, *U.P.B. Sci. Bull., Series A*. 2016; 78(2):1-10.
3. Eringen AC. Theory of micropolar fluids, *J. Math. Anal. Appl.* 1966; 16:1-18.
4. Eringen AC. Theory of thermo-microfluids, *J. Math. Anal. Appl.* 1972; 38:480-496.
5. Fatunmbi EO, Okoya SS. Electromagnetohydrodynamic micropolar-Casson fluid boundary layer flow and heat transfer over a stretching material featuring temperature-based thermophysical properties in a porous medium, *Journal of the Nigerian Mathematical Society*. 2021; 40(3):245-268.
6. Fatunmbi EO, Ogunseye HA, Sibanda P. Magnetohydrodynamic micropolar fluid flow in a porous medium with multiple slip conditions, *International Communications in Heat and Mass Transfer*. 2020; 115:104577.
7. Fatunmbi EO, Adeniyani A. MHD stagnation point-flow of micropolar fluid past a permeable stretching plate in porous media with thermal radiation, chemical reaction and viscous dissipation. *J Adv Math Comp Sci*. 2018; 26(1):1-19.
8. Fatunmbi EO, Okoya SS. Heat transfer in boundary layer magneto-micropolar fluids with temperature-dependent material properties over a stretching sheet. *Adv Mater Sci Eng*, 2020, 1-11.
9. Fatunmbi EO, Okoya SS, Makinde OD. Convective Heat Transfer Analysis of Hydromagnetic Micropolar Fluid Flow Past:an Inclined Nonlinear Stretching Sheet with Variable Thermophysical Properties, *Diffusion Foundations*. 2019; 26:63-77.
10. Gumber P, Yaseen M, Rawat K, Kumar M. Heat transfer in micropolar hybrid nanofluid flow past a vertical plate in the presence of thermal radiation and suction/injection effects, *Partial Differential Equations in Applied Mathematics*. 2022; 5:100240.
11. Hsiao KL. Combined Electrical MHD Heat Transfer Thermal Extrusion System Using Maxwell Fluid with Radiative and Viscous Dissipation Effects. *Appl Therm Eng*. Elsevier Ltd, 2016. Doi: 10.1016/j.applthermaleng.2016.08.208



12. Jabeen K, Mushtaq M, Akram RM. Analysis of the MHD Boundary Layer Flow over a Nonlinear Stretching Sheet in a Porous Medium Using Semi Analytical Approaches, *Mathematical Problems in Engineering*, 2020, Article ID 3012854, 1-9.
13. Jain S, Gupta P. Entropy Generation Analysis of MHD Viscoelasticity-Based Micropolar Fluid Flow Past a Stretching Sheet with Thermal Slip and Porous Media, *Int. J. Appl. Comput. Math.* 2019; 5:61. Doi: <https://doi.org/10.1007/s40819-019-0643-x>
14. Kamel MT, Roach D, Hamdan MH. On the Micropolar Fluid Flow through Porous Media Proceedings of the 11th WSEAS Int. Conf. on Mathematical Methods, Computational Techniques and Intelligent Systems. 2014; 11:1-9.
15. Khan U, Mohyud-Din ST, Bin-Mohsin B. Convective heat transfer and thermo-diffusion effects on flow of nanofluid towards a permeable stretching sheet saturated by a porous medium. *Aerosp Sci Technol.* 2016; 50:19603.
16. Khan SA, Nie Y, Ali A. Multiple Slip Effects on Magnetohydrodynamic Axisymmetric Buoyant Nanofluid Flow above a Stretching Sheet with Radiation and Chemical Reaction, *Symmetry.* 2019; 11:1171. Doi: 10.3390/sym11091171
17. Lukaszewicz G. *Micropolar fluids: theory and applications.* 1st ed. Boston: Birkhauser, 1999.
18. Lund LA, Omar Z, Khan I. Mathematical analysis of magnetohydrodynamic (MHD) flow of micropolar nanofluid under buoyancy effects past a vertical shrinking surface: dual solutions. *Heliyon.* 2019; 5(9):1-10.
19. Makinde OD, Khan WA, Khan ZH. Buoyancy effects on MHD stagnation point flow and heat transfer of a nanofluid past a convectively heated stretching/shrinking sheet. *Int J Heat Mass Transf.* 2015; 62:52633.
20. Nagaraju G, Murthy JVR. Unsteady flow of a micropolar fluid generated by a circular cylinder subject to longitudinal and torsional oscillations *Theoret. Appl. Mech.* 2014; 41(1):71-91.
21. Rashad AR, Khan WA, EL-Kabeir SMM, EL-Hakiem MA. Mixed Convective Flow of Micropolar Nanofluid across a Horizontal Cylinder in Saturated Porous Medium, *Appl. Sci.* 2019; 9:5241. Doi: 10.3390/app9235241
22. Tripathy RS, Dash GC, Mishra SR, Hoque MM. Numerical analysis of hydromagnetic micropolar fluid along a stretching sheet embedded in porous medium with non-uniform heat source and chemical reaction, *Eng. Sci. Technol.* 2017; 19:1573-1581.
23. Upreti H, Pandey AK, Kumar M. MHD flow of ag-water nanofluid over a flat porous plate with viscous-ohmic dissipation, suction/injection and heat generation/absorption. *Alexandria Eng J.* 2018; 57(3):1839-1847. Doi: <http://dx.doi.org/10.1016/j.aej.2017.03.018>.